



Exploration of synthetic antioxidant flavonoid analogs as acetylcholinesterase inhibitors: an approach towards finding their quantitative structure–activity relationship

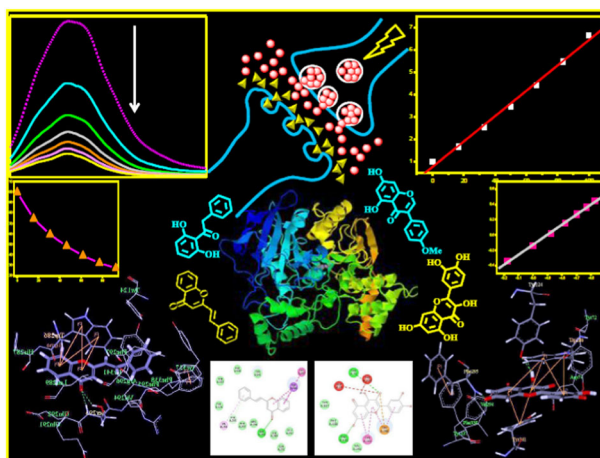
Abhijit Karmakar¹ · Pravin Ambure² · Tamanna Mallick¹ · Sreeparna Das¹ · Kunal Roy² · Naznin Ara Begum ¹

Received: 23 December 2018 / Accepted: 13 March 2019
© Springer Science+Business Media, LLC, part of Springer Nature 2019

Abstract

The binding interactions between acetylcholinesterase (AChE) and a series of antioxidant flavonoid analogs were studied by fluorescence spectroscopic assay. The present study incorporated different classes of naturally occurring and synthetic flavonoid compounds like flavones, isoflavones, and chalcones as well as a few standard antioxidants. The AChE inhibitory (AChEI) activity of these compounds was further analyzed using *in silico* techniques, namely pharmacophore mapping, quantitative structure–activity relationship (QSAR) analysis, and molecular docking studies. We have also compared the AChE inhibitory and radical scavenging antioxidant activities of these compounds. Both the AChE inhibitory and antioxidant activities of these compounds were found to be highly dependent on their structural patterns. However, it was observed that, in general, flavones are comparatively better AChE inhibitors as well as antioxidants compared to chalcones.

Graphical Abstract



Supplementary information The online version of this article (<https://doi.org/10.1007/s00044-019-02330-8>) contains supplementary material, which is available to authorized users.

✉ Kunal Roy
kunal.roy@jadavpuruniversity.in
✉ Naznin Ara Begum
naznin.begum@visva-bharati.ac.in

¹ Department of Chemistry, Siksha-Bhavana, Visva-Bharati (Central University), Santiniketan 731235 West Bengal, India
² Drug Theoretics and Cheminformatics Laboratory, Department of Pharmaceutical Technology, Jadavpur University, Kolkata 700032 West Bengal, India

Keywords Flavonoids · Acetylcholinesterase inhibitory activity · Antioxidant · QSAR · In silico method

Introduction

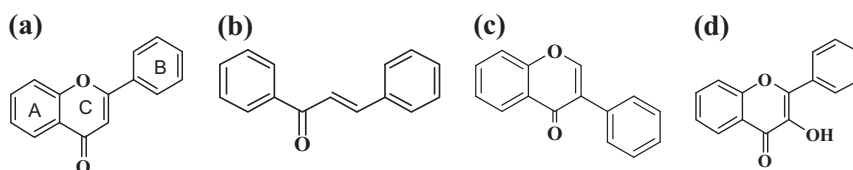
Among the various age-related neurodegenerative diseases, Alzheimer's disease (AD) is the most prevalent one, and it is a common cause of dementia, progressive memory loss, and several other cognitive impairments in elderly people (Uriarte-Pueyo and Calvo 2011; Bartolini et al. 2003; Xie et al. 2014; Balkis et al. 2015; Pinho et al. 2013; Malisauskas et al. 2015; Luo et al. 2013; Kung et al. 2001; Förstl and Kurz 1999; Kamal et al. 2014). Scientists are still working on the etiology of the AD. There are two major hypotheses associated with the origin of this disease. According to the cholinergic hypothesis, factors like lowering of the concentration of acetylcholine (ACh), a cholinergic neurotransmitter in the synaptic gap is responsible for AD (Pinho et al. 2013; Luo et al. 2013; Mesulam et al. 2002; Racchi et al. 2004). On the other hand, as per the amyloid cascade hypothesis, abnormalities in the protein functions, e.g., formation of the β -amyloid fibrils and tau-protein aggregations are the causes of neural brain cell death in AD patients (Pinho et al. 2013; Luo et al. 2013; Mesulam et al. 2002; Racchi et al. 2004). Formation of β -amyloid fibrils is also found to be associated with other age-associated neurodegenerative diseases, e.g., Parkinson's and Huntington's diseases (Pinho et al. 2013; Malisauskas et al. 2015). One of the major causes of the decrease in the concentration of ACh in the synaptic gap is its hydrolytic degradation, catalyzed by the enzyme, acetylcholinesterase (AChE). Therefore, inhibiting AChE enzyme helps in increasing or retaining the concentration of ACh. Also, AChE itself may promote the formation of neurotoxic amyloid fibrils associated with AD (Li et al. 2013).

Various reactive oxygen species (ROS) play a crucial role in the signaling pathways, but an excessive production of ROS due to impaired cellular metabolism causes a disturbance in living cell's own defense and repair mechanisms (Reyes et al. 2004; Pietta 2000). This produces oxidative stress, which damages living cells. Recent reports on the etiology of AD indicate that the oxidative stress accelerates the lipid peroxidation of the membrane components of neural cells, which causes the dysfunction of the brain cells and ultimately the death of brain cells occurs in people suffering from AD (Reyes et al. 2004). In addition to this, oxidative stress is also found responsible for the neurotoxicity related to the abnormal aggregation of β -amyloid peptides (Reyes et al. 2004). With the progress of age, this harmful effect becomes more prominent and initiates various age-associated neurodegenerative diseases, like AD. Thus, oxidative stress plays a very crucial role in the brain

cell damage of the elderly people suffering from AD (Reyes et al. 2004). Therefore, from this discussion, it is clearly evident that AD is multi-factorial in nature and there is no single cause for the pathology of AD, rather there are various possible causes among which factors like (i) diminished level of ACh due to its degradative hydrolysis catalyzed by AChE, (ii) formation of β -amyloid and other neurotoxic fibrils in the synapses, and (iii) oxidative stress are very crucial. However, each of these causes is inter-related with each other. Scientists tried to develop drugs for the treatment of AD patients by targeting these factors and the most successful class of inhibitors, i.e., acetylcholinesterase inhibitors (AChEIs) are widely used. The conventional AChEIs are either alkaloid type natural products or synthetic compounds having scaffolds of a natural product. Examples of such AChEIs (used as anti-AD drugs) are galanthamine, rivastigmine, and donepezil, etc. (Uriarte-Pueyo and Calvo 2011; Williams et al. 2011). However, these drugs only provide symptomatic treatment, they are also not free from toxic side effects, e.g., insomnia, gastrointestinal and hepatotoxic disorders found in AD patients treated with these drugs (Uriarte-Pueyo and Calvo 2011). Till now, no such multifunctional drugs are available which can fight against all the probable causes of AD (discussed earlier) simultaneously. Hence, the researchers are in a continuous search to find out such multifunctional AD drugs. We have already discussed that AChE inhibitors are beneficial in AD treatment but the compounds showing dual property, i.e., anti-oxidant and AChE inhibition property are prone to be more efficient in the treatment of AD.

Natural products, like flavonoids (especially poly-hydroxy flavones) are well known as plant-derived antioxidants (Leung et al. 2006; Silva et al. 2002; Vitorino and Sottomayor 2010). These nutraceuticals are the part of human dietary supplements and as the antioxidants, they primarily reduce oxidative stress in living cells. Thus, they show wide-spectrum of protective and remedial effects towards various age-related cerebrovascular and neurodegenerative diseases, like Parkinson's disease and AD (Leung et al. 2006; Silva et al. 2002; Vitorino and Sottomayor 2010; Chigurupati et al. 2018). Flavonoids (both naturally occurring and synthesized) are reported to show AChE inhibitory activities (Uriarte-Pueyo and Calvo 2011; Xie et al. 2014; Balkis et al. 2015; Pinho et al. 2013; Luo et al. 2013; Sun et al. 2018). Luo et al. (2013) have explained the in vitro anti AChE and butyrylcholine esterase (BChE) activities of a series of 4-dimethylflavone analogs. They also showed that flavonoids having AChEI and BChEI activities can also prevent the aggregation of

Fig. 1 Structure of flavonoids.
a Flavone: parent compound;
b chalcone; **c** isoflavone; and
d 3-hydroxyflavone



β -amyloid peptides. Malisauska et al. (2015) showed that flavonoids are potent inhibitors for insulin amyloid-like fibril formation. These reported data clearly indicate the potential of flavonoids as multifunctional anti-AD drugs. Therefore, it is highly essential to understand the AChE inhibitory potential of such flavonoid-based antioxidants, which will be helpful to develop non-toxic multifunctional anti-AD drugs in the future. This motivated us to perform the present study.

Nature (mainly the plant family) is the source of the wide spectrum of bioactive scaffolds under the flavonoid class. In fact, flavonoids represent one of the most diverse and widespread classes of plant-derived natural products which include chalcones, flavones, and isoflavones etc., and all the compounds under this class have a common $C_6-C_3-C_6$ system, i.e., they all have the parent structure consisting of two aromatic rings (A and B) linked by 3-carbons which are the parts of an oxygenated heterocyclic ring as shown in Fig. 1 (Geissman 1962; Harborne and Mabry 1982).

Structures of these compounds precisely control their bioactivities. Besides the naturally occurring flavonoids, a large number of flavonoids and their analogs can also be synthesized in the laboratory by employing very easy synthetic techniques (Das et al. 2014; Alam and Mostahar 2005; Desideri et al. 1998; Balasubramanian and Nair 2000). This surely eliminates the tedious process of isolation of these compounds from plants. Very often, these compounds are potentially beneficial as antioxidants and besides that, they have a wide range of bioactivities, which are mainly regulated by their structural characteristics (Das et al. 2014; Alam and Mostahar 2005; Desideri et al. 1998; Balasubramanian and Nair 2000). Thus, these molecules can be ideal candidates for understanding the relationship between structure and AChE inhibitory activities. However, systematic studies involving all types of flavonoids to develop their quantitative structure–activity relationship (QSAR) [for AChEI activity] have not been done exhaustively, and only very few works are reported on flavonoids as multifunctional AChEIs (Xie et al. 2014; Luo et al. 2013; Sun et al. 2018).

In the present work, we have designed and synthesized a series of different classes of antioxidant flavonoid analogs (mainly flavones, 3-hydroxyflavones, isoflavones, and chalcones), and along with some standard antioxidants, we have tested their AChE binding interactions and inhibitory activities by fluorescence spectrophotometric titration

method (Xie et al. 2014; Ryu et al. 2014). A total of 30 compounds were tested for their AChEI activity (Table 1).

The results were further explored using in silico techniques, such as, pharmacophore mapping, QSAR model development (Das et al. 2014; Brahmachari et al. 2015), and molecular docking studies. Later, we have extended this work to compare the AChE inhibitory and radical scavenging antioxidant activities of the tested compounds, which may be helpful in the future to develop antioxidant flavonoid-based multifunctional and non-toxic anti-AD drugs.

Materials and methods

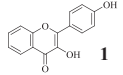
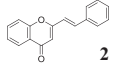
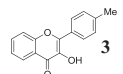
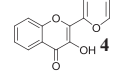
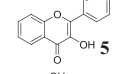
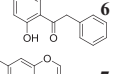
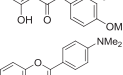
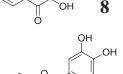
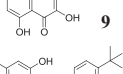
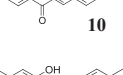
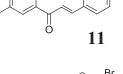
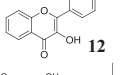
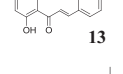
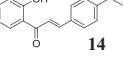
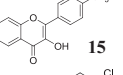
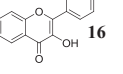
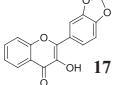
General experimental

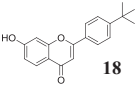
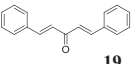
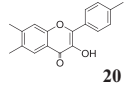
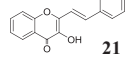
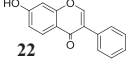
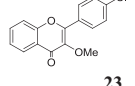
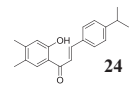
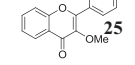
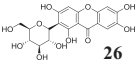
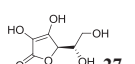
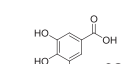
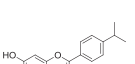
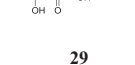
Electric eel (*Electrophorus electricus*) acetylcholinesterase (AChE) [Type-VI-S, EC 3.1.1.7, Sigma-Aldrich (MO, USA)] and all other reagents (either A.R. or M.B. grade) including standard antioxidants, trolox, gallic acid, ascorbic acid, and quercetin (E. Merck and SRL, India) were used as obtained without any further purification. However, the purity of each reagent was checked routinely by thin layer chromatography (TLC). Solvents used in the present study were of spectroscopic grade. Milli-Q (Milli-Q Academic with 0.22 mm Millipack R40) water was used as per requirement.

Synthesis of test compounds (antioxidant flavonoid analogs)

A total of 30 compounds were tested for their AChEI activity. Among these 30 test compounds used for the present study, (7, 9, 22, 26–28, 30) were purchased from Sigma-Aldrich (MO, USA) and (3–5, 8, 14, 16–18, 21) (Table 1) were synthesized previously in our laboratory (Das et al. 2014). Compounds (1–2, 10–13, 15, 19–20, 23–25, 29) were synthesized presently according to the reported methods (Das et al. 2014; Alam and Mostahar 2005; Desideri et al. 1998; Balasubramanian and Nair 2000) (Scheme 1). The synthesized test compounds were purified by repeated crystallization, and the purity of these compounds was routinely checked by TLC which was carried out in silica gel GF₂₅₄ pre-coated plates using DCM (dichloromethane) or DCM and petroleum ether (60–80 °C)

Table 1 Acetylcholinesterase inhibitory (AChEI) and DPPH radical scavenging antioxidant activities of flavonoid analogs

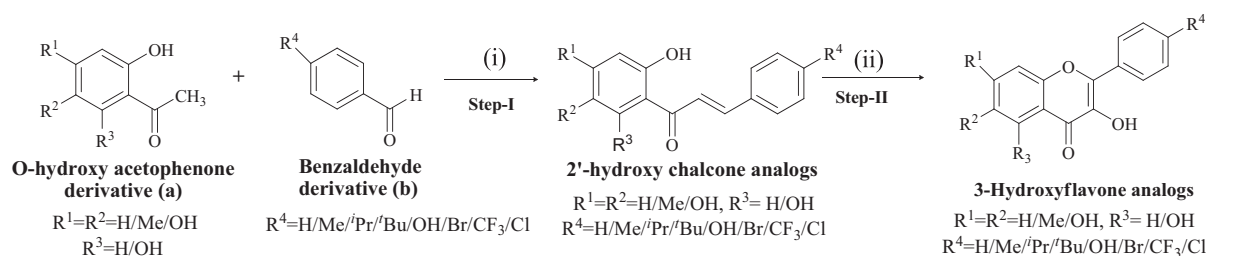
Compound	$K_{sv} \pm s.d.$ (Stern-Volmer constant)	K_q (Quenching rate constant)	$K_B \pm s.d.$ (Binding constant)	$n \pm s.d.$ (No. of binding site)	AChEI ($EC_{50} \pm s.d.$) (μM)	DPPH radical scavenging antioxidant activity [($EC_{50} \pm s.d.$) (mM)]
 1	0.08±0.09	7.70×10^{12}	$1.28 \times 10^6 \pm 0.01$	1.27±0.01	15.5±0.5	0.01±0.001
 2	0.13±0.05	1.30×10^{13}	$1.25 \times 10^5 \pm 0.02$	0.99±0.02	8.3±0.3	1419.93±240.38
 3	0.05±0.09	4.90×10^{12}	$8.85 \times 10^4 \pm 0.04$	1.06±0.04	23.5±1.1	$0.005 \pm 8.5 \times 10^{-05}$
 4	0.04±0.04	3.70×10^{12}	$1.36 \times 10^4 \pm 0.03$	0.91±0.03	27.9±0.8	0.03±0.002
 5	0.05±0.02	5.30×10^{12}	$4.11 \times 10^4 \pm 0.02$	0.98±0.02	19.5±0.4	0.38±0.004
 6	0.09±0.15	8.70×10^{12}	$7.32 \times 10^5 \pm 0.02$	1.21±0.02	15.2±0.4	0.74±0.02
 7	0.11±0.15	1.06×10^{13}	$2.74 \times 10^6 \pm 0.02$	1.31±0.02	12.8±0.4	160.38±8.73
 8	0.06±0.18	5.70×10^{12}	$3.20 \times 10^5 \pm 0.03$	1.19±0.03	24.6±1.0	0.02±0.001
 9	0.11±0.12	1.14×10^{13}	$1.00 \times 10^6 \pm 0.02$	1.17±0.02	11.3±0.4	$0.01 \pm 9.6 \times 10^{-05}$
 10	0.05±0.11	4.50×10^{12}	$6.59 \times 10^4 \pm 0.03$	1.04±0.03	25.5±1.3	19.57±0.63
 11	0.01±0.60	8.00×10^{11}	$6.05 \times 10^3 \pm 0.06$	0.97±0.06	125.1±3.5	1.65±0.006
 12	0.04±0.12	3.50×10^{12}	$6.65 \times 10^4 \pm 0.03$	1.07±0.03	33.4±0.6	0.93±0.006
 13	0.01±0.02	1.20×10^{12}	$1.03 \times 10^4 \pm 0.01$	0.98±0.01	83.9±3.1	0.32±0.002
 14	0.03±0.11	2.80×10^{12}	$1.12 \times 10^5 \pm 0.02$	1.15±0.02	44.7±1.5	17.11±0.39
 15	0.97±0.03	9.70×10^{13}	$1.12 \times 10^4 \pm 0.10$	0.98±0.10	20.9±1.0	1.23±0.13
 16	0.01±0.04	1.40×10^{12}	$6.99 \times 10^3 \pm 0.03$	0.98±0.03	74.9±2.7	0.66±0.02
 17	0.002±0.08	2.00×10^{11}	$4.84 \times 10^2 \pm 0.04$	0.82±0.04	591.5±52.2	0.09±0.004

	0.04±0.16	4.20 X 10 ¹²	1.69X10 ⁵ ±0.01	1.16±0.01	31.5±1.0	44.29±2.05
	0.02±0.09	1.90 X 10 ¹²	3.39X10 ³ ±0.01	0.81±0.01	39.8±2.3	71.84±3.68
	0.009±0.01	9.00 X 10 ¹¹	6.05X10 ³ ±0.05	0.97±0.05	125.1±4.3	4.94±0.13
	0.03±0.07	3.00 X 10 ¹²	6.30X10 ⁴ ±0.02	1.08±0.02	38.1±1.6	0.04±0.001
	0.02±0.05	2.30 X 10 ¹²	7.83X10 ⁴ ±0.01	1.13±0.01	47.0±1.7	37.35±5.69
	0.01±0.01	8.00 X 10 ¹¹	2.42X10 ³ ±0.03	0.75±0.03	122.3±2.3	5.85±1.36
	0.01±0.04	1.40 X 10 ¹²	3.45X10 ⁴ ±0.01	1.09±0.01	74.6±1.3	5568.74±7.25
	0.01±0.04	5.00 X 10 ¹¹	1.17X10 ⁴ ±0.01	1.10±0.01	199.21±2.4	30.58±5.46
	0.04±0.01	4.20 X 10 ¹²	1.51X10 ⁶ ±0.04	1.40±0.04	40.98±1.0	0.007±0.001
	0.01±0.02	9.00 X 10 ¹¹	9.46X10 ³ ±0.01	1.00±0.01	109.62±1.8	0.033±0.001
	0.23±1.09	2.29 X 10 ¹³	3.14X10 ⁷ ±0.08	1.50±0.08	10.54±0.4	0.011±0.0002
	0.001±0.03	1.00 X 10 ¹¹	13.6±0.01	0.47±0.01	Not found	29.60±1.75
	1.82X10 ⁻⁴ ±0.01	1.80 X 10 ¹⁰	5.55±0.02	0.45±0.02	Not found	0.012±0.0001

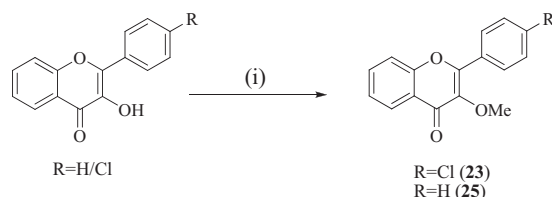
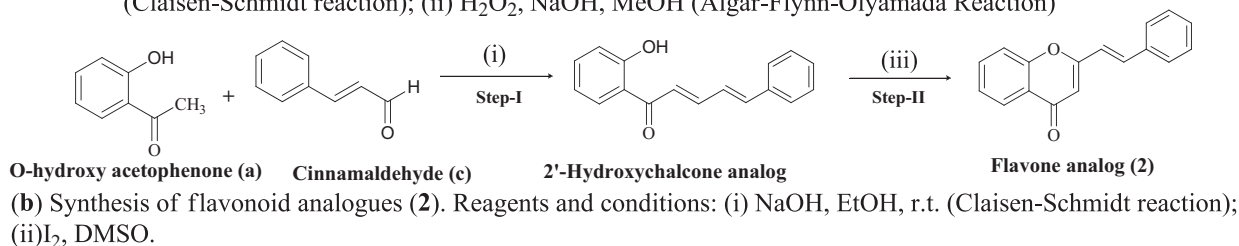
mixture as eluting solvents. Silica gel (100–200 mesh) was used for column chromatography. The structures of the synthesized compounds were confirmed on the basis of melting point, ¹H NMR and ¹³C NMR spectral and literature data. Melting points were checked by an electrothermal apparatus and were uncorrected. ¹H NMR and ¹³C NMR spectra of the test compounds were recorded at 400 MHz and also at 300 MHz in Bruker AVANCE-400 and Bruker AVANCE-300 NMR spectrometers using either CDCl₃ or DMSO-*d*₆ as solvents and tetramethylsilane (TMS) as the internal standard.

Synthesis of test compounds (1, 2, 10–13, 15, 20, 23–25)

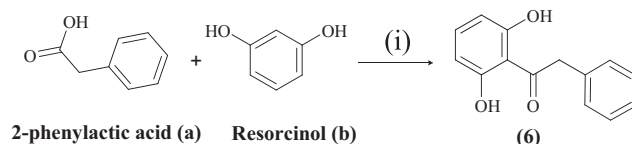
At first, 2'-hydroxychalcones with desired substitution patterns were prepared by Claisen–Schmidt reaction using appropriately substituted acetophenone (*o*-hydroxyacetophenone) (**a**) and benzaldehyde derivatives (**b**) as the starting materials. These 2'-hydroxychalcone derivatives thus synthesized were employed to prepare various flavone analogs as shown in Scheme 1 (Das et al. 2014; Alam and Mostahar 2005; Desideri et al. 1998). In case of (**2**), in place of benzaldehyde derivative, cinnamaldehyde was used



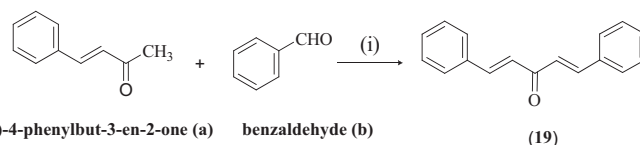
(a) Synthesis of flavonoid analogues (**1-2**, **10-13**, **15**, **20**, **24**). Reagents and conditions: (i) NaOH, EtOH, r.t. (Claisen-Schmidt reaction); (ii) H_2O_2 , NaOH, MeOH (Algar-Flynn-Oyamada Reaction)



(c) Synthesis of (**23**) and (**25**). Reagents and conditions: (i) Me_2SO_4 , KOH, dry acetone.



(d) Synthesis of (**6**). Reagents and conditions: (i) BF_3 , Et_2O at $85^\circ C$.



(e) Synthesis of (**19**). Reagents and conditions: (i) NaOH at $25^\circ C$.

Scheme 1 Synthesis of flavonoid analogs (**1**), (**2**), (**10-13**), (**15**), (**19-20**), (**23-25**) (Das et al. 2014, Alalm and Mostahar 2005; Desideri et al. 1998; Begum et al. 2011)

(Begum et al. 2011). 3-hydroxyflavone analogs (**23**) and (**25**) were synthesized by the methylation of the 3-OH group of corresponding flavone analog as shown in Scheme 1 (Das et al. 2014; Alam and Mostahar 2005; Desideri et al. 1998; Begum et al. 2011).

In step 1, 2'-hydroxychalcone analogs were prepared following reported methods (Das et al. 2014; Alam and Mostahar 2005; Desideri et al. 1998). In general, appropriate KOH (2.5 mmol) was added to a solution of appropriately substituted 2-hydroxyacetophenone derivative (**a**) (1 mmol) in EtOH (5 mL) and the reaction mixture was stirred continuously. It was kept in cold condition for

15 min and then, it was again stirred at room temperature for 15 min. After this substituted benzaldehyde derivative (**b**) (1 mmol) was added to it and the reaction mixture was stirred continuously until the starting material was fully consumed (checked by TLC). After that, the reaction mixture was cooled in an ice bath and acidified (pH ~2) with HCl. The solid product was obtained which was filtered and washed with water. The crude product was purified by repeated crystallization in MeOH medium.

In step 2, these 2'-hydroxychalcone analogs were used to synthesize corresponding 3-hydroxyflavone analogs following reported methods (Das et al. 2014; Alam and Mostahar 2005;

Desideri et al. 1998). In general, 2'-hydroxychalcone analogs with appropriate substitution pattern (2 mmol) was dissolved in MeOH (5 mL) followed by the addition of KOH (2.5 equiv, 5 mmol) and H₂O₂ solution (30%, 0.8 mL) under stirring condition at 0–5 °C. The reaction mixture was then stirred for another 8 h at 0–5 °C. Then the reaction mixture was stirred at RT for another 16 h. The reaction mixture was diluted with water and acidified with 2 M HCl. The precipitate was filtered, washed with enough cold water, and recrystallized from ethanol.

For the synthesis of (2), corresponding 2'-hydroxychalcone analog with appropriate substitution pattern (30 mmol) obtained in the above method was dissolved in DMSO (25 mL) and crystalline iodine (30 mmol) was added to it. The reaction mixture was refluxed for 20 min and then it was diluted with water whereby a solid product was obtained. It was filtered off and washed with 20% aq. sodium thiosulphate solution. The crude product was recrystallized from ethanol (Das et al. 2014; Alam and Mostahar 2005).

3-Hydroxyflavone analogs (23) and (25) were synthesized according to the reported method

Here, a brief description is given. *p*-Chloro-3-hydroxyflavone (0.87 mmol) synthesized by previously discussed method was dissolved in 5 mL dry acetone followed by cautious addition of solid KOH (1.31 mmol) and dimethyl sulphate (1.05 mmol) in small portions. The temperature was kept at 25 °C. After that, the reaction mixture was refluxed for 1 h. The completion of the reaction was checked by TLC. Then, the reaction mixture was washed with water several times to make it acid-free. The organic part was extracted with ethyl acetate. This process was repeated 4 times. Finally, the organic parts containing the methylated product (23 and 25) were collected and the solvent was evaporated under reduced pressure whereby a solid product was obtained. This was filtered, washed with enough cold water, and recrystallized from ethanol (Desideri et al. 1998).

Synthesis of test compound (6)

(6) was obtained during the synthesis of isoflavone analog. The method (Balasubramanian and Nair 2000) followed for this synthesis is shown in Scheme 1. A mixture of phenylacetic acid (a) (100 mg, 1 equiv, 1.66 mmol), resorcinol (b) (182.75 mg, 1 equiv, 1.66 mmol) and BF₃·Et₂O (0.64 mL, 5.15 mmol) was refluxed at 85 °C for 90 min with continuous stirring. The reaction mixture was cooled to room temperature and then poured into aqueous NaOAc solution (100 mL, 10%). Then, it was washed with water and followed by brine solution. After that, it was extracted with ethyl acetate. This process was repeated 4 times and collected organic parts were dried over Na₂SO₄. The solvent was removed by evaporation

under vacuum. The crude product was subjected to column chromatography using silica gel and 10–12% ethyl acetate in petroleum ether as an eluent whereby pure (6) was obtained (Balasubramanian and Nair 2000).

Test compound (19) was synthesized by reported method (Furniss et al. 1984) as shown in Scheme 1

Here, the general methods were given. However, slight modifications were needed to be done for individual compounds as per the experimental requirements. Structures of the products were confirmed on the basis of ¹H and ¹³C NMR data as well as by comparing the reported melting point (m.p.) data.

Characterization of test compounds

3-Hydroxy-2-(4-hydroxyphenyl)-4H-chromen-4-one (1)

Pale yellow solid (0.24 g, 47%): m.p. 282–286 °C; ¹H NMR (400 MHz, DMSO-*d*₆): δ (ppm) 10.09 (1H, s); 9.31 (1H, s); 8.10 (3H, t, *J* = 13.6 Hz); 7.80–7.72 (2H, m); 7.47–7.43 (1H, m); 6.94 (2H, d, *J* = 8.8 Hz) (Tyukavkina and Pogodaeva 1971).

(E)-2-styryl-4H-chromen-4-one (2)

Pale yellow solid (0.079 g, 47%): m.p. 132–133 °C; ¹H NMR (400 MHz, CDCl₃): δ (ppm) 8.22 (1H, dd, *J* = 1.6, 8 Hz); 7.73–7.69 (1H, m); 7.69–7.61 (3H, m); 7.56 (1H, d, *J* = 8.4 Hz); 7.47–7.39 (3H, m); 6.82 (1H, d, *J* = 16 Hz); 6.36 (1H, s) (Gomes et al. 2009).

3-Hydroxy-2-*p*-tolyl-4H-chromen-4-one (3)

Yellow needle shaped crystals (0.045 g, 42.4%): m.p. 135–136 °C; ¹H NMR (300 MHz, CDCl₃): δ (ppm) 8.24 (1H, d, *J* = 6.6 Hz); 8.15 (2H, d, *J* = 8.4 Hz); 7.68 (1H, t, *J* = 6.9 Hz); 7.58 (1H, d, *J* = 8.33 Hz); 7.42 (1H, t, *J* = 6.9 Hz); 7.34 (2H, d, *J* = 6.6 Hz); 3.46 (1H, brs); 2.42 (3H, s) (Das et al. 2014).

2-(Furan-2-yl)-3-hydroxy-4H-chromen-4-one (4)

Brown needle shaped crystals (0.023 g, 22.3%): m.p. 190–192 °C; ¹H NMR (300 MHz, CDCl₃): δ (ppm) 8.28 (1H, d, *J* = 8 Hz); 7.74 (1H, d, *J* = 5.6 Hz); 7.72 (1H, t, *J* = 8.4 Hz, *J* = 8.4 Hz); 7.64 (1H, d, *J* = 8.2 Hz); 7.45 (1H, t, *J* = 7.6 Hz, *J* = 7.6 Hz); 7.38 (1H, d, *J* = 3.2 Hz); 7.01 (1H, brs); 6.69 (1H, t, *J* = 3.6 Hz, *J* = 3.6 Hz) (Das et al. 2014).

3-Hydroxy-2-phenyl-4H-chromen-4-one (5)

Off-white crystalline solid (0.059 g, 55.2%): m.p. 170 °C; ¹H NMR (300 MHz, CDCl₃): δ (ppm) 8.26–8.29 (3H, m);

7.74 (1H, t, $J = 8.6$ Hz, $J = 8.6$ Hz); 7.626 (1H, d, $J = 8.6$ Hz); 7.55 (3H, m); 7.43 (1H, t, $J = 7.8$ Hz, $J = 7.8$ Hz); 7.03 (1H, brs) (Das et al. 2014).

1-(2,6-Dihydroxyphenyl)-2-phenylethanone (6)

Brown solid (0.326 g, 31.5%): m.p. 168 °C; ^1H NMR (400 MHz, CDCl_3): δ (ppm) 12.68 (1H, s); 7.75 (1H, d, $J = 8.8$ Hz); 7.38–7.34 (3H, m); 7.29 (2H, dd, $J = 6.4$ Hz, $J = 4.4$ Hz); 6.41 (2H, dd, $J = 8$ Hz, $J = 5.6$ Hz); 5.94 (1H, brs); 4.23 (2H, s) (Balasubramanian and Nair 2000).

2-(4-(Dimethylamino)phenyl)-3-hydroxy-4H-chromen-4-one (8)

Brown needle shaped crystals (0.067 g, 64%): m.p. 190–191 °C; ^1H NMR (400 MHz, $\text{DMSO}-d_6$): δ (ppm) 9.18 (1H, s); 8.15 (2H, d, $J = 8.8$ Hz); 8.1 (1H, dd, $J = 7.6$ Hz); 7.72–7.76 (2H, m); 7.44 (1H, t, $J = 6.8$ Hz, $J = 6.8$ Hz); 6.87 (2H, d, $J = 9.2$ Hz); 3.03 (6H, s) (Das et al. 2014).

(E)-3-(4-tert-butylphenyl)-1-(2,4-dihydroxyphenyl)prop-2-en-1-one (10)

Brown solid (0.685 g, 63%): m.p. 168–170 °C; ^1H NMR (400 MHz, CDCl_3): δ (ppm) 13.44 (1H, s); 7.86 (2H, dd, $J = 15.6$, $J = 8.8$ Hz); 7.59 (2H, d, $J = 8.4$ Hz); 7.54 (1H, d, $J = 15.6$ Hz); 7.45 (2H, t, $J = 8.8$ Hz); 6.45 (2H, t, $J = 8$ Hz); 5.9 (1H, brs); 1.33 (9H, s).

(E)-1-(2-hydroxy-4,5-dimethylphenyl)-3-p-tolylprop-2-en-1-one (11)

Pale yellow solid (0.454 g, 55.8%) m.p. 81–82 °C; ^1H NMR (400 MHz, CDCl_3): δ (ppm) 12.73 (1H, s); 7.87 (1H, d, $J = 15.6$ Hz); 7.62 (2H, d, $J = 1.6$ Hz); 7.57 (2H, t, $J = 8$ Hz); 7.24 (1H, d, $J = 8$ Hz); 6.82 (1H, s); 2.40 (3H, s); 2.28 (3H, s); 2.26 (3H, s) (Naik and Naik 1990).

2-(4-Bromophenyl)-3-hydroxy-4H-chromen-4-one (12)

Pale yellow solid (0.282 g, 54.4%): m.p. 171–173 °C; ^1H NMR (400 MHz, CDCl_3): δ (ppm) 8.28 (1H, d, $J = 1.6$ Hz); 8.27–8.15 (2H, m); 7.77–7.72 (1H, m); 7.71–7.67 (2H, m); 7.61 (1H, d, $J = 8.4$ Hz); 7.47–7.43 (1H, m); 7.08 (1H, brs) (Gunduz et al. 2012).

(E)-3-(4-isopropylphenyl)-1-(2,4,6-trihydroxyphenyl)prop-2-en-1-one (13)

Brown solid (0.416 g, 47.2%): m.p. 260–263 °C; ^1H NMR (400 MHz, CDCl_3): δ (ppm) 7.93 (1H, dd, $J = 1.6$, 8 Hz);

7.56 (1H, dd, $J = 1.6$, 7.2 Hz); 7.55–7.50 (2H, m); 7.34 (2H, d, $J = 8$ Hz); 7.10 (1H, t, $J = 15.2$ Hz); 7.04 (1H, d, $J = 8.4$ Hz); 6.00 (2H, s); 5.60 (1H, brs); 5.12 (1H, d, $J = 12.4$ Hz); 4.67 (1H, d, $J = 12.4$ Hz); 2.96 (1H, t, $J = 14$ Hz); 1.28 (6H, d, $J = 6.8$ Hz).

(E)-3-(4-tert-Butylphenyl)-1-(2-hydroxyphenyl) prop-2-en-1-one (14)

Yellow crystalline solid (0.156 g, 76.3%): m.p. 83–84 °C; ^1H NMR (400 MHz, CDCl_3): δ (ppm) 12.87 (1H, s); 7.95 (1H, d, $J = 6.4$ Hz); 7.94 (1H, d, $J = 15$ Hz); 7.65 (1H, d, $J = 15.2$ Hz); 7.63 (2H, d, $J = 8.4$ Hz); 7.52 (1H, t, $J = 7.2$ Hz); 7.47 (2H, d, $J = 8.4$ Hz); 7.04 (1H, d, $J = 8.4$ Hz); 6.97 (1H, t, $J = 6.8$ Hz, $J = 6.8$ Hz); 1.35 (9H, s) (Das et al. 2014).

3-Hydroxy-2-(4-(trifluoromethyl)phenyl)-4H-chromen-4-one (15)

White solid (0.141 g, 27.3%): m.p. 164–165 °C; ^1H NMR (400 MHz, CDCl_3): δ (ppm) 8.39 (2H, d, $J = 8$ Hz); 8.26 (1H, dd, $J = 8.4$ Hz, $J = 1.6$ Hz); 7.78 (2H, d, $J = 8.8$ Hz); 7.76–7.72 (1H, m); 7.61 (1H, d, $J = 8.8$ Hz); 7.47–7.43 (1H, m); 7.19 (1H, brs) (Itoh et al. 1986).

2-(4-Chlorophenyl)-3-hydroxy-4H-chromen-4-one (16)

Yellow needle shaped crystal (0.074 g, 55.75%): m.p. 162–164 °C; ^1H NMR (400 MHz, CDCl_3): δ (ppm) 8.27 (1H, d, $J = 8$ Hz); 8.23 (2H, d, $J = 8.8$ Hz); 7.75 (1H, t, $J = 7.2$ Hz, $J = 7.2$ Hz); 7.6 (1H, d, $J = 8.4$ Hz); 7.52 (2H, d, $J = 8.4$ Hz); 7.45 (2H, t, $J = 7.6$ Hz, $J = 7.6$ Hz); 7.08 (1H, brs) (Das et al. 2014).

2-(Benzo[d][1,3]dioxol-5-yl)-3-hydroxy-4H-chromen-4-one (17)

Pale yellow needle shaped crystals (0.055 g, 52.75%): m.p. 207–208 °C; ^1H NMR (400 MHz, CDCl_3): δ (ppm) 8.27 (1H, d, $J = 8$ Hz); 7.9 (1H, d, $J = 8.4$ Hz); 7.80 (1H, d, $J = 1.6$ Hz); 7.74 (1H, t, $J = 6.8$ Hz, $J = 6.8$ Hz); 7.6 (1H, d, $J = 8.4$ Hz); 7.45 (1H, t, $J = 7.2$ Hz, $J = 7.2$ Hz); 7.03 (1H, brs); 7.01 (1H, d, $J = 8.4$ Hz); 6.09 (2H, s) (Das et al. 2014).

2-(4-tert-Butylphenyl)-7-hydroxy-4H-chromen-4-one (18)

Pale yellow solid (0.035 g, 35%): m.p. 82 °C; ^1H NMR (400 MHz, CDCl_3): δ (ppm) 8.04 (1H, d, $J = 8.8$ Hz); 7.4 (2H, d, $J = 8$ Hz); 7.35 (1H, s); 7.34 (1H, s); 7.26 (1H, d, $J = 5.6$ Hz); 7.25 (2H, d, $J = 8.4$ Hz); 6.57 (1H, s); 1.3 (9H, s) (Das et al. 2014).

3-Hydroxy-6,7-dimethyl-2-p-tolyl-4H-chromen-4-one (20)

Brownish yellow solid (0.408 g, 77.6%): m.p. 140–142 °C; ^1H NMR (400 MHz, CDCl_3): δ (ppm) 7.66 (1H, s); 7.35 (2H, d, $J = 8$ Hz); 7.23 (2H, d, $J = 8$ Hz); 6.83 (1H, s); 2.37 (3H, s); 2.25 (3H, s); 2.19 (3H, s).

3-Hydroxy-2-styryl-4H-chromen-4-one (21)

Yellow needle shaped crystals (0.099 g, 94%): m.p. 191–192 °C: ^1H NMR (300 MHz, CDCl_3): δ (ppm) 8.24 (1H, d, $J = 6$ Hz); 7.72 (1H, t, $J = 6.6$ Hz, $J = 6.6$ Hz); 7.65 (2H, d, $J = 6$ Hz); 7.58 (1H, d, $J = 6.3$ Hz); 7.57 (1H, d, $J = 9.6$ Hz); 7.45 (1H, t, $J = 6.6$ Hz, $J = 6.6$ Hz); 7.43 (2H, d, $J = 6.3$ Hz); 7.4 (1H, d, $J = 11.7$ Hz); 7.38 (1H, d, $J = 11.7$ Hz); 6.57 (1H, brs) (Das et al. 2014).

2-(4-chlorophenyl)-3-methoxy-4H-chromen-4-one (23)

Gray solid (0.273 g, 52.3%): m.p. 112–114 °C; ^1H NMR (400 MHz, CDCl_3): δ (ppm) 8.26 (1H, dd, $J = 1.6$ Hz, $J = 8$ Hz); 8.07 (2H, dd, $J = 2$, 6.8 Hz); 7.71–7.66 (1H, m); 7.54 (1H, s); 7.52–7.48 (2H, m); 7.42–7.38 (1H, m); 3.90 (3H, s) (Dhoubhadel et al. 1981).

(E)-1-(2-hydroxy-4,5-dimethylphenyl)-3-(4-isopropylphenyl) prop-2-en-1-one (24)

Yellow solid (0.571 g, 67.8%): m.p. 81–82 °C; ^1H NMR (400 MHz, $\text{DMSO}-d_6$): δ (ppm) 12.75 (1H, s); 7.91 (1H, d, $J = 15.6$ Hz); 7.62 (4H, t, $J = 15.6$ Hz); 7.31 (2H, t, $J = 20$ Hz); 6.84 (1H, s); 3.00–2.92 (1H, m); 2.29 (6H, d, $J = 9.6$ Hz); 1.31 (3H, s); 1.29 (3H, s).

3-Methoxy-2-phenyl-4H-chromen-4-one (25)

Green solid (0.361 g, 68.4%): m.p. 158–160 °C; ^1H NMR (400 MHz, CDCl_3): δ (ppm) 8.29 (1H, dd, $J = 8$ Hz, $J = 1.6$ Hz); 8.14–8.11 (2H, m); 7.70–7.68 (1H, m); 7.57–7.53 (4H, m); 7.42 (1H, t, $J = 8$ Hz); 3.99 (3H, s) (Das et al. 2016).

3,5,7-Trihydroxy-2-(4-isopropylphenyl)-4H-chromen-4-one (29)

Pale yellow solid (0.404 g, 43.6%): m.p. 288–292 °C; ^1H NMR (400 MHz, CDCl_3): δ (ppm) 7.59 (1H, d, $J = 8.4$ Hz); 7.41 (3H, t, $J = 14.8$ Hz); 7.01 (1H, brs); 6.25 (1H, s); 5.98 (1H, s); 5.40 (1H, brs); 5.18 (1H, s); 2.99 (1H, t, $J = 14$ Hz); 1.30 (6H, d, $J = 7.2$ Hz).

In vitro acetylcholinesterase inhibitory (AChEI) activity assay of flavonoid analogs by fluorescence spectroscopic techniques

The inhibitory interactions of flavonoid analogs and other test compounds with AChE were studied by fluorescence spectroscopy. AChE has a characteristic excitation maximum [$\lambda_{\text{max(ex)}}$] at 280 nm, whereas it shows an emission maximum [$\lambda_{\text{max(em)}}$] at a wavelength of 335 nm, on its excitation at 280 nm. In the presence of a ligand (which can bind with AChE and inhibits its activity), the fluorescence of AChE was found to be quenched (Xie et al. 2014; Ryu et al. 2014; Santillo and Liu 2015). This phenomenon was exploited to study the binding interactions between a ligand and AChE and we have followed the methods of Xie et al. (2014) and Ryu et al. (2014) to study the AChEI activity of the test compounds. However, to apply these methods in the present case, modifications were done as per the requirements.

The fluorescence emission spectra of AChE in the absence and presence of different concentrations of test compounds were recorded individually to study the inhibitory or binding activity of the test compounds with AChE. Here, a typical experimental procedure is given (Xie et al. 2014; Brahmachari et al. 2015).

At first, stock solutions (1 or 10 mM) of each of the test compounds [1–30] were prepared in EtOH. In a typical AChE inhibitory interaction study, 1 mL of AChE (5 U mL^{-1}) in 0.2 M phosphate buffer (PBS, pH 8.0) solution (3.0 mL) was taken in the 1.0 cm quartz cuvette and titrated spectro-fluorometrically by the successive addition of the test compound solution. Fluorescence emission spectra of all the experimental solutions were recorded in a PerkinElmer spectrophotometer of model no. LS55 in the wavelength range of 300–450 nm with an excitation wavelength (λ_{ex}) of 276 nm and the slit width was fixed at 10 nm for both excitation and emission beams. For each of the test compounds, the fluorescence intensity of the experimental solution was noted at its emission maximum [$\lambda_{\text{em(max)}}$ 335–339 nm]. This was further used to determine the effective concentration (EC_{50}) of the test compound showing 50% AChE inhibitory activity (method of calculation of EC_{50} is discussed in the later section).

All the fluorescence measurements were done at 25 °C and we have observed that the spectra of all the test solutions remained unchanged for a long time during which the experiments were done. Hence, we can safely rule out the possibility of photo-decomposition of the experimental samples which may give errors in the results. The final concentration of EtOH in the test solution was negligible (<1%).

Radical scavenging antioxidant activity assay of flavonoid analogs

The *in vitro* antioxidant activity of the test compounds was evaluated by measuring their ability to scavenge the free radical 1,1-diphenyl-2-picryl hydrazyl radical (DPPH). The method of Koleva et al. (2002) was followed to measure the DPPH radical scavenging activity of the test compounds (1–2, 6–7, 10–13, 15, 19–20, 22–26, and 29). However, some modifications (Das et al. 2014) were needed to be done to apply the method in the present case. For test compounds (3–5, 8–9, 14, 16–18, 21, 27–28 and 30), we cited the previously reported data (Das et al. 2014).

DPPH free radical scavenging activity was calculated by using the following formula (Das et al. 2014; Koleva et al. 2002):

$$\text{Free radical scavenging activity (\%)} = \left[\frac{(\text{Abs}_{\text{Control}} - \text{Abs}_{\text{Sample}})}{\text{Abs}_{\text{Control}}} \right] \times 100$$

The test compound concentration showing 50% radical inhibition activity (EC_{50}) was calculated from the plot of % DPPH free radical scavenging activity against the test compound concentration.

Computational strategies for the AChE inhibitory activity profiling of flavonoid analogs

Pharmacophore screening of flavonoid analogs

The pharmacophore model (Fig. 2) used for mapping all the 30 compounds (1–30) under evaluation was previously developed using the Discovery Studio software (Discovery Studio 2007) and already reported by one of our groups (Ambure et al. 2014). Eighty-five compounds with experimentally determined bioactivity values against human AChE enzyme (ranging from 0.950 to 11,587.77 nM) were employed for developing this model. The model (Fig. 2) comprises four features, namely, two hydrogen bond acceptors (i.e., HBA1 and HBA2), one hydrophobic (HYD) aliphatic, and one HYD aromatic feature, present at specific relative distances. The HBA feature signifies the regions favorable for hydrogen bond acceptor groups, while the HBA feature vector indicates the direction of hydrogen bond formation. The HYD aliphatic feature implies the regions favorable for aliphatic hydrophobic group's substitution, while the HYD aromatic feature signifies the region favorable for aromatic hydrophobic groups. All the 30 compounds (1–30) were screened through this pharmacophore using the ligand mapping protocol available in the Discovery Studio software. The geometric fit values were computed for all the compounds, where a fit value tells how

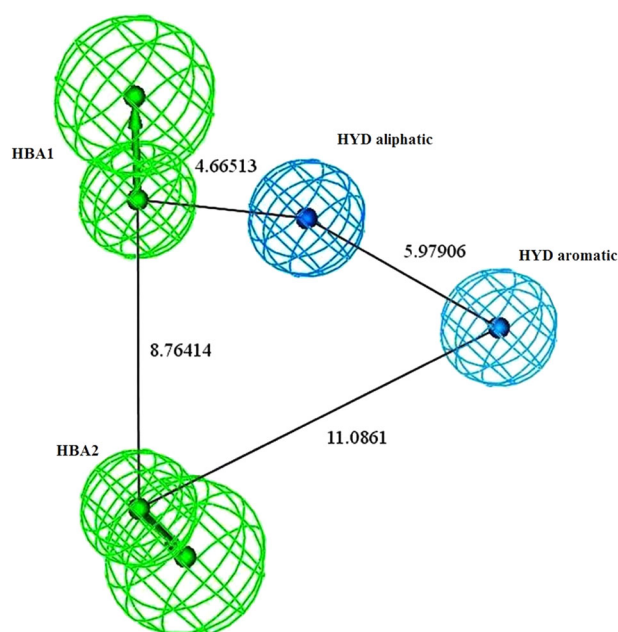


Fig. 2 The pharmacophore model (Ambure et al. 2014) comprising 4 pharmacophoric features, i.e., hydrogen bond acceptor 1 (HBA1), HBA2, hydrophobic (HYD) aliphatic, and HYD aromatic feature [Reproduced with permission from the Publisher.]

well the chemical sub-structures of a compound match the location constraints of the pharmacophoric features and their distance deviation from the feature centers (Rella et al. 2006). For every molecule, 100 conformers were allowed to generate, while the threshold energy value was set to 20 kcal/mol. For screening the compounds, the “Maximum Omitted Features” was set to two.

Molecular docking studies to understand the interaction of flavonoid analogs with AChE

The LigandFit docking module available in Discovery Studio software (Discovery Studio 2007) was used to perform the docking studies between the 30 compounds under study and the human AChE enzyme. The crystal structure of human AChE (PDB ID: 4M0E) was downloaded from protein data bank (PDB) database. Further, the protein was prepared via inserting missing atoms in incomplete residues, modeling missing loop regions, deleting alternate conformations (disorder), adding hydrogens, removing waters, standardizing atom names, etc., and energy minimization was performed using the CHARMM forcefield. The ligands (i.e., all 30 compounds) were also prepared by generating canonical tautomers, enumerating isomers, enumerating ionization states at a given pH range, and generating 3D conformations. Ligand conformations were generated using Monte-Carlo algorithm. The docking protocol was validated by first docking the co-crystal ligand (dihydrotanshinone I)

into the active site of human AChE enzyme (PDB ID: 4M0E). For a valid docking protocol, the root mean square deviation (RMSD) between the actual conformation present in the protein structure and the docked conformation of co-crystal ligand should be low. Also, the docked conformation should show similar intermolecular interactions that are reported in the human AChE co-crystal structure. Once the protocol was set, the same protocol was employed for docking all 30 compounds under study. During the process, top 10 conformations were retained, evaluated and ranked using the selected scoring functions. Here, LigScore1, LigScore2, Piecewise Linear Potential 1 (PLP1), Piecewise Linear Potential 2 (PLP2), Jain and Potential of mean force (PMF) were used as the scoring functions.

Development of quantitative structure–activity relationship models for AChEI activity of flavonoid analogs

The set comprising 28 compounds (since the activity values of **29** and **30** are not defined) was employed to build a QSAR model. The AChE inhibitory activity values of all the 28 compounds expressed as EC₅₀ values (μM) were converted to negative logarithm of EC₅₀ (pEC₅₀) values. Note that prior to conversion to pEC₅₀, the EC₅₀ values in micromolar units were converted into molar units. All the chemical structures were drawn using the Marvin Sketch software (<http://www.chemaxon.com/products.html>). The descriptors were calculated using Cerius version 410, Dragon software 6 (Mauri et al. 2006), and PaDEL-Descriptor version 2.1 (Yap 2011) software tools. The total pool of descriptors includes different classes such as electrotopological state keys, electronic, topological, constitutional, functional group counts spatial, structural, thermodynamic, and extended topochemical atom (ETA) indices. Further, data pretreatment was performed to remove constant (variance cut-off < 0.0001) and inter-correlated (correlation coefficient cut-off ≥ 0.99) descriptors using an in-house developed DataPreTreatment 1.2 software available at http://teqip.jdvu.ac.in/QSAR_Tools/. Since there were a limited number of compounds available for performing QSAR study, all 28 compounds were employed in the training set for model development. Here, the model was developed exploiting several chemometric techniques like stepwise multiple linear regression (stepwise MLR) (DTC laboratory software tools freely available at http://teqip.jdvu.ac.in/QSAR_Tools/), genetic function approximation (GFA), GFA-spline (Cerius2 Version 410). Moreover, for validation of the developed model, different statistical internal validation metrics were calculated such as correlation coefficient (r^2), adjusted r^2 (r^2 adjusted), standard error of estimate (SEE), leave- n -out (L- n -O) cross-validated correlation coefficients (in this study, Q^2_{L-1-O} , Q^2_{L-2-O} , Q^2_{L-3-O} , Q^2_{L-4-O} , Q^2_{L-5-O}), and $^cR^2_p$ based on Y-randomization test results. The Y-randomization

test checks the robustness of the developed model. In this test, the activity values of the training set compounds are randomly shuffled keeping the descriptor matrix unchanged, and new models are built based on the shuffled activity values.

Results and discussion

Synthesis of flavonoid analogs and their DPPH radical scavenging antioxidant activity

In the present work, we have explored the AChE inhibitory activity of a series of flavonoid analogs (**1–26**, **29**) along with some standard antioxidants (**27–28**, **30**) which showed appreciable in vitro antioxidant activity as measured by the 1,1-diphenyl-2-picryl hydrazyl radical (DPPH) radical scavenging assay (Das et al. 2014) (Table 1). We have synthesized this flavonoid series by varying their structural pattern, e.g., by changing the nature, number and position of the substituent(s) on Ring-A, B, or C or by altering the conjugation profile of the parent flavone skeleton (Fig. 1). For a better comparison purpose, wide varieties of antioxidant flavonoid analogs were selected. Compounds used for the present study were both naturally occurring (**7**, **9**, and **26**) and synthesized flavonoid analogs (**1–6**, **8**, **10–25**, and **29**). From the structural point of view, these compounds belong to different classes of flavonoids, like chalcones (**10–11**, **13**, **14**, **19**, and **24**), flavones (**1–5**, **8–9**, **12**, **15–18**, **20–21**, **23**, **25–26**, and **29**), and isoflavones (**7**, **22**) along with their intermediate product (**6**) (Table 1).

For the present work, we have studied the DPPH radical antioxidant activity of the test compounds, (**1**), (**2**), (**6**), (**7**), (**10–13**), (**15**), (**19–20**), (**22–26**), and (**29**) and compared to that of the test compounds, (**3–5**), (**8–9**), (**14**), (**16–18**), (**21**), (**27–28**), and (**30**) for which we cited the previously reported data (Das et al. 2014). In general, 3-hydroxyflavone analogs showed higher DPPH radical scavenging antioxidant activity than chalcone analogs. It is interesting to note that, the presence of various electron releasing groups at 4'-position of Ring-B of 3-hydroxyflavone analogs appreciably enhanced the activity as it was observed earlier (Das et al. 2014). The antioxidant activity of flavonoid analogs highly depends on the structural pattern, i.e., number, nature, and position of substituent(s) on Ring-A, B, and C, geometry and other physico-chemical parameters of these molecules (Das et al. 2014).

Fluorescence spectroscopic studies on the binding interactions between the flavonoid analogs and AChE

Fluorescence spectroscopy-based analytical methods have wide applications in various biomedical and other technological fields due to their high sensitivity, specificity, and

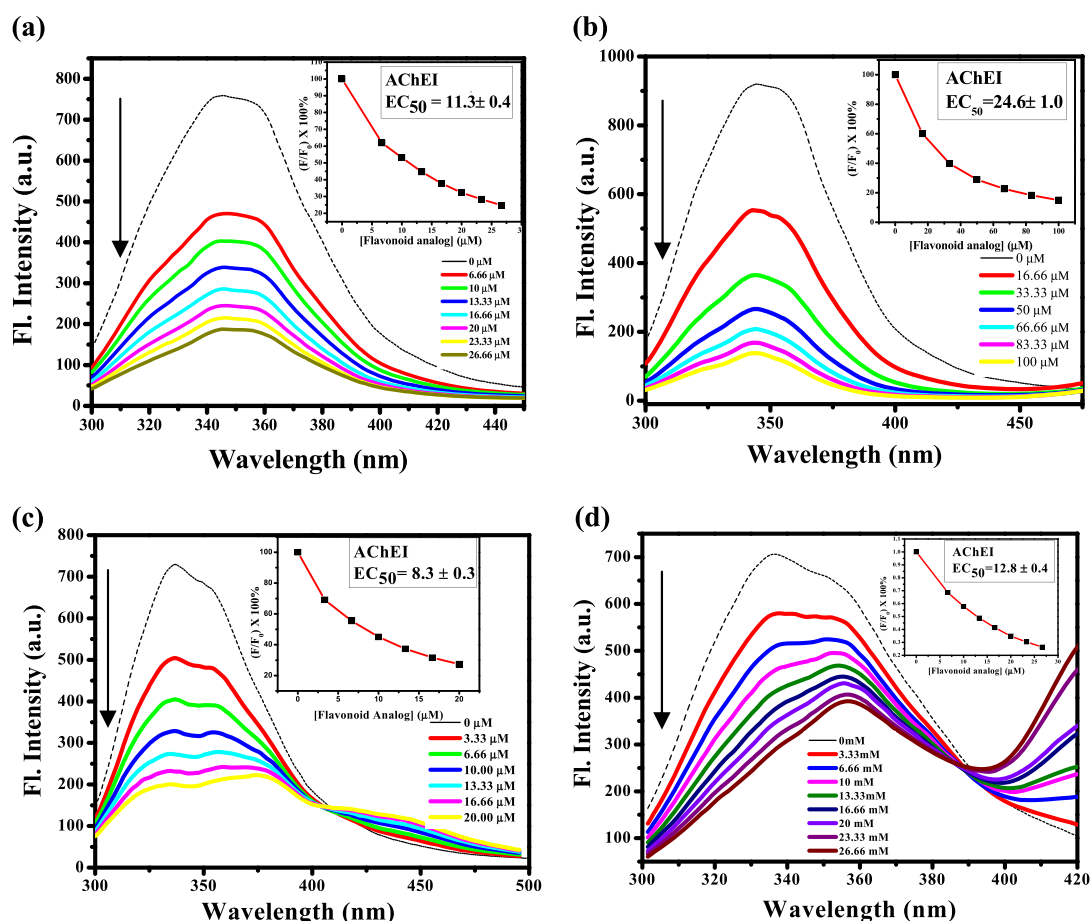


Fig. 3 Fluorescence emission spectra of AChE in the absence (indicated by dashed line) and presence of flavonoid analogs (**9**) **a**, (**8**) **b**, (**2**) **c**, and (**7**) **d** having different concentrations in phosphate buffer (pH = 7.4) at 25 °C. The excitation wavelength (λ_{ex}) was 280 nm. The

direction of arrow indicates the quenching of fluorescence of AChE on gradual addition of flavonoid analogs. The changes of % AChE inhibitory activity ($F/F_0 \times 100$) of flavonoid analogs with the change of their concentrations are shown in corresponding insets

accuracy. In the present case, we have exploited the intrinsic fluorescence behavior of AChE to assay the inhibitory activity of the samples towards it. We have adopted the methods of Xie et al. (2014) and Ryu et al. (2014) to measure the AChEI activities of the samples.

The intrinsic fluorescence activity of AChE is due to the presence of tryptophan, tyrosine, and phenylalanine amino acid residues in its structure and the fluorescence emission spectrum of AChE shows a broad emission maximum at 335 nm upon its excitation at 280 nm. Fluorescence emission spectra of AChE in the absence and presence of different concentration of each of the samples were recorded individually and here, the fluorescence emission spectra of AChE in the absence and presence of four structurally different flavonoid analogs, (**9**), (**8**), (**2**), and (**7**) [Table 1], are shown in Fig. 3a–d.

The same experiment was repeated with other flavonoid samples (Table 1). In each case, on gradual addition of sample solution to AChE, a significant decrease of its

fluorescence emission intensity was observed. This spectroscopic feature was found to be common in all the cases in addition to these four representatives (**9**, **8**, **2**, and **7**). AChE showed this intense change in its fluorescence spectral behavior due to the change of its micro-environment which is related to the extent of its binding interactions with flavonoid analogs. A careful examination of Fig. 3a–d indicates similar changes (quenching) of fluorescence behavior of AChE in the presence of different flavone analogs, like (**9**) and (**8**) (Fig. 3a, b). However, the fluorescence quenching behavior was found to be totally different in the presence of (**2**) which has a conjugation pattern different from earlier two flavone analogs (Fig. 3c). Again, in case of isoflavone type of compound, (**7**), which have different structural pattern, we have observed a totally different fluorescence behavior of AChE (Fig. 3d).

It was interesting to note that though the quenching of AChE fluorescence was found to be common in all the cases, the nature of fluorescence spectra of AChE (i.e., peak

position and intensity) in the presence of all of these samples was not the same.

The fluorescence activity of any fluorophore is very sensitive towards the changes of its microenvironment. One of the major causes triggering such a change in the microenvironment of a fluorophore is its binding interactions with some other species, which in the present case are flavonoid analogs. On the other hand, the extent of binding interactions, i.e., mode and strength of binding between a fluorophore (e.g., AChE) and a quencher, like the flavonoids as in the present case depends on their structural complementarities. In the present case, the structural patterns of the quenchers were varied, whereas the structure of the fluorophore remains unaltered throughout the study and we have observed various changes in the fluorescence quenching pattern of AChE (Fig. 3a–d) as discussed earlier. Changes in the fluorescence pattern (quenching) of AChE were also observed in the case of other sample compounds (Table 1). From these data, it is clearly evident that the drastic changes (quenching) of the fluorescence intensity of the fluorophore AChE in the presence of the fluorescence quencher like antioxidant flavonoid analogs certainly confirm the binding interactions between these two species, and the mode/extent of binding between the flavonoid analogs and AChE is mainly controlled by the structural pattern of these test compounds.

We have also determined the EC_{50} values which denote the concentration of the flavonoid and other samples required for the 50% quenching of fluorescence of AChE. This indirectly indicates the 50% inhibition of activity of AChE due to its binding interaction with flavonoid samples. The fluorescence intensities of AChE [at λ_{em} (max) 335 nm] were monitored for the different concentrations of the flavonoid samples.

The % of fluorescence quenching of AChE, i.e., % inhibition of activity of AChE is denoted by the following equation:

$$\% \text{ Inhibition of activity of AChE} = F/F_0 \times 100\% \quad (1)$$

where the initial and final fluorescence intensities are indicated by F_0 and F , respectively.

The EC_{50} values of flavonoid analogs and other samples were calculated from the plot of % inhibitory activity vs. concentration of the test samples. The plots are shown in the insets of Fig. 3a–d. The EC_{50} values calculated from the plots are given in Table 1. The same protocol was used to calculate the pEC_{50} values of all other compounds and the results are given in Table 1. In general, chalcone has higher EC_{50} values over flavone type of compounds. However, some chalcones like (10) and (14) have shown lower EC_{50} values, i.e., higher AChEI activity like flavones. In case of flavone type of compounds (17), (20), (23), and (25), higher

EC_{50} values, i.e., lower AChEI activity was observed. It is interesting to note that generally an increase in the number of hydroxyl groups on the parent flavones or chalcone moieties increased their AChEI activity as in the case of compounds (7), (9), (10), (18), and (26). On the other hand, incorporation of the conjugated part in the core structure of these compounds also increased their activity as in the case of compounds (2), (19), and (21). In addition to these, the presence of bulky electron releasing group at the 4' position of Ring-B also enhanced the AChEI activity of flavones type of compounds. It was also observed that the replacement of benzene ring (Ring-B) by furan moiety increased the AChEI activities of both flavones and chalcone type of compounds, e.g., (4).

Quenching of the fluorescence intensity of AChE during its interaction with a fluorescence quencher may be the outcome of several processes, like excited state energy transfer or ground state formation etc. (Xie et al. 2014; Bera et al. 2008; Kanakis et al. 2007). According to the mechanistic pathway, these processes are categorized into two types: dynamic and static fluorescence quenching processes (Kanakakis et al. 2007; Zhang et al. 2011; Lu et al. 2010). To understand the mechanistic pathway involved in the quenching of fluorescence of AChE during its interaction with antioxidant flavonoid analogs, we have applied classical Stern–Volmer equation for quenching (Lu et al. 2010; Jana et al. 2012) as shown here:

$$F_0/F = 1 + K_{SV} \quad (2)$$

where F_0 and F are the fluorescence intensities of AChE in the absence and presence of the quencher, i.e., samples having different concentrations. The concentrations of the test samples is denoted by $[E]$ and K_{SV} is the Stern–Volmer constant.

The values of the Stern–Volmer constant, K_{SV} and quenching rate constant, K_q are used as the guiding tool to determine the fluorescence quenching pathway (Xie et al. 2014). Stern–Volmer plots (F_0/F vs. $[E]$) for four different flavonoid analogs (9, 8, 2, and 7) are shown in Fig. 4a–d. The Stern–Volmer fluorescence quenching constant, K_{SV} are obtained as $0.11 \pm 0.12 \text{ M}^{-1}$ for (9) and $0.06 \pm 0.18 \text{ M}^{-1}$ for (8). For (2), the K_{SV} value was obtained as $0.13 \pm 0.05 \text{ M}^{-1}$ and for (7), the K_{SV} was calculated as $0.11 \pm 0.15 \text{ M}^{-1}$. Therefore, from the Stern–Volmer analysis, it is evident that the substituent as well as the conjugation pattern of flavonoid analogs have strong influence on their fluorescence quenching activity towards AChE.

The K_{SV} and K_q ($K_q = K_{SV}/\tau_0$, when τ_0 is the average fluorescence lifetime of fluorophore, like AChE) values for all the flavonoids analogs and other test samples are shown in Table 1. The quenching rate constants, K_q for these species varied within the range of 10^{10} – $10^{13} \text{ L mol}^{-1} \text{ s}^{-1}$.

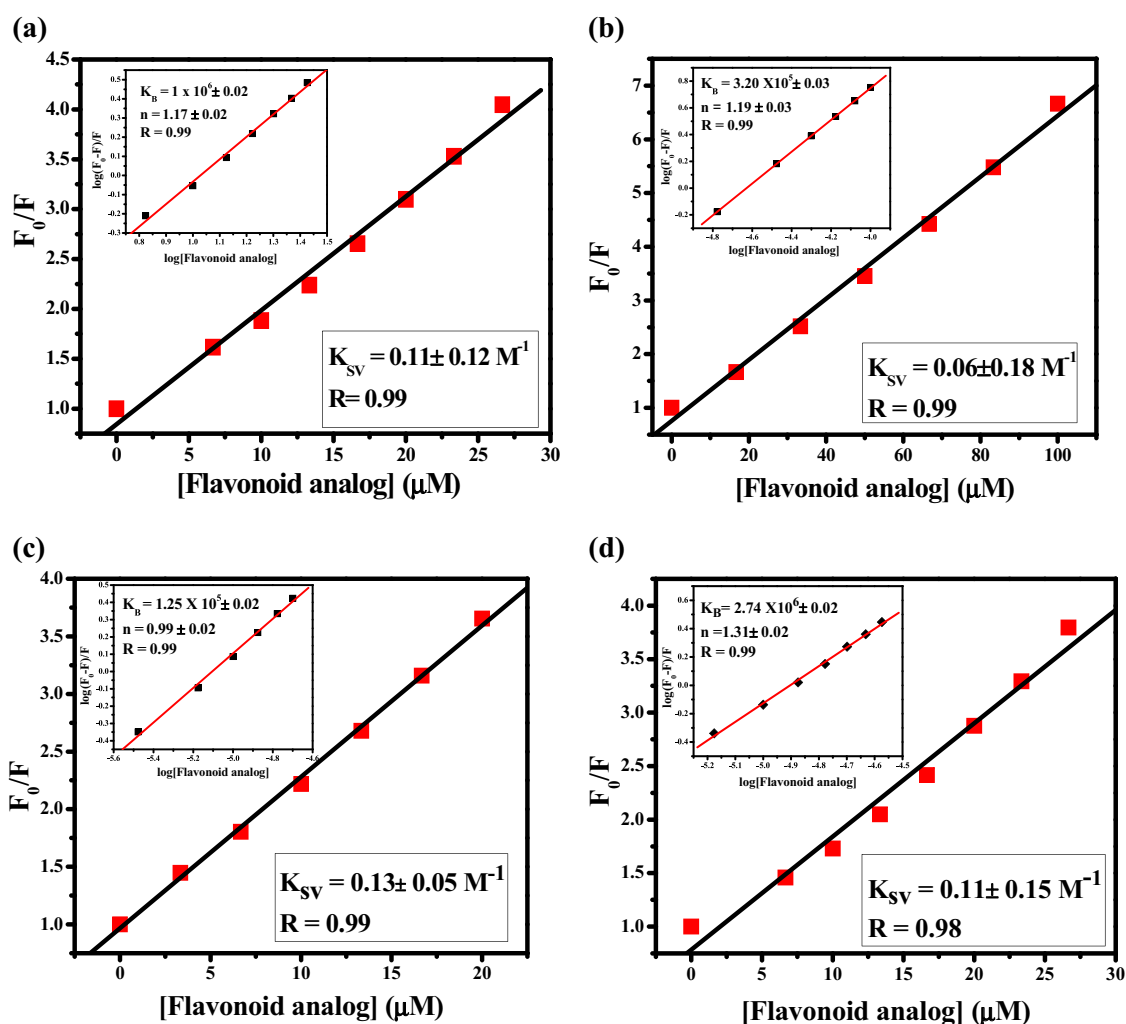


Fig. 4 Stern–Volmer plots for the quenching of the fluorescence emission intensity of AChE in the presence of different flavonoid analogs: (9) **a**, (8) **b**, (2) **c**, and (7) **d**. Insets of these figures represent

the plot of $\log[(F_0 - F)/F]$ vs. $\log[\text{flavonoid analog}]$, binding constants (K_B) and number of binding sites (n)

The K_q values obtained for the present set of flavonoid analogs indicate the static quenching of fluorescence of AChE by flavonoid analogs which is possibly due to the formation of flavones–AChE complex (Xie et al. 2014). The nature of binding interactions between AChE and flavonoid analogs was further studied by monitoring the changes of the fluorescence intensities of AChE at λ_{em} (max) 335 nm and these data were used to calculate the binding constant, K_B and n (no. of binding sites) for such interactions by applying the following equation (Liu et al. 2010):

$$\log(F_0 - F)/F = \log K_B + n \log[E] \quad (3)$$

where F_0 and F are the fluorescence intensities of AChE at λ_{em} (max) 335 nm in the absence and presence of different concentrations of flavonoid analogs and other samples ($[E]$). The results for four structurally different flavonoid analogs are shown in the insets of Fig. 4a–d. In each case, the $\log K_B$

was calculated from the linear plot of $\log[(F_0 - F)/F]$ vs. $\log[E]$. The values of K_B are found to vary in the range of 10^4 – 10^6 M^{-1} , whereas, n varies with the range of 0.99–1.19 (insets of Fig. 3a–d). Similar results are observed for all other samples tested for the present study. These K_B values further support the formation of flavones–AChE complex may be associated with static fluorescence quenching mechanism (Xie et al. 2014).

Binding affinities of flavonoids towards AChE regulate their AChEI activities and EC_{50} values were helpful to understand and compare the AChEI activities of these compounds. Binding affinities of such compounds towards AChE were found to be increased with the increase of their K_B values (Xie et al. 2014). Thus flavonoid analogs having K_B values were expected to be better AChE inhibitors. In the present case also, in general, AChEI activities of flavonoids were found to be increased with the increase of

their K_B values. However, there were some exceptions (Table 1).

In summary, we can say that the structural pattern of flavonoid analogs mainly influenced their AChEI activity. So, in the next step, we were interested to understand the correlation between their structures and their AChEI activity. For this, we have performed computational studies using the methods discussed earlier.

In silico studies on the AChE inhibitory (AChEI) profiling of flavonoid analogs: quantitative structure–activity relationship (QSAR) analysis of flavonoid analogs

The AChE inhibitory (AChEI) activities of the flavonoid analogs, as measured by fluorometric assays were further analyzed to understand the structural requirements of such molecules for showing appreciable AChEI activities. A QSAR model (Das et al. 2014; Ryu et al. 2014) was developed to suggest a lead structure and it might help designing novel AChEI inhibitors based on flavonoid scaffold by optimizing the lead structure. The EC_{50} values of the samples (as shown in Table 1) were correlated with the structural features of the flavonoid analogs by the utilization of suitable molecular descriptors. The final QSAR model was obtained using the genetic functional approximation (GFA)-spline technique (Das et al. 2014; Ryu et al. 2014). The acceptability of the developed QSAR model was evaluated using appropriate internal validation metrics. The internal validation metrics ($r^2 = 0.683$, $r^2_{\text{(adjusted)}} = 0.643$, $SEE = 0.259$) including the $L-n-O$ cross-validation results indicate significant predictive potential of the developed QSAR model. The Y randomization results (Average $r^2 = 0.107$, average $Q^2_{L-1-O} = -0.242$, $^cR^2_p = 0.641$) for 50 randomly generated models further confirm the robustness of the QSAR model. The GFA spline equation with standardized values of regression coefficients is given below and contribution of each descriptor present in the final model is described in detail.

Standardized GFA Spline Equation :

$$\begin{aligned} pEC_{50} = & 4.396(\pm 0.049) + 0.207(\pm 0.06)SC - 3.C \\ & - 0.232(\pm 0.051)<S_{ssO} - 5.935> \\ & + 0.317(\pm 0.059)<0.201 - ETA_EtaP_L> \end{aligned}$$

Internal validation metrics :

$$r^2 = 0.683, r^2_{\text{(adjusted)}} = 0.643, SEE = 0.259, F = 17.23 (DF : 3, 24)$$

Cross – validation results :

$$\begin{aligned} Q^2_{L-1-O} &= 0.589, Q^2_{L-2-O} = 0.584, Q^2_{L-3-O} \\ &= 0.579, Q^2_{L-4-O} = 0.573; Q^2_{L-5-O} = 0.567. \end{aligned}$$

Y-randomization test results (for 50 random models) :

$$\text{Average } r^2 = 0.107, \text{ average } Q^2_{L-1-O} = -0.242, ^cR^2_p = 0.641.$$

Descriptor contribution

SC-3_C

This descriptor belongs to the class of Kier & Hall subgraph count index (SC). Here, SC-3_C counts the number of clusters of third order. It designates the amount of branching present in a molecule. It positively contributes to the activity and hence according to this descriptor, if we increase branching, the activity will improve. This can be observed in compounds **9**, **10**, **15**, **18**, where the number of clusters is high, and correspondingly the activity is better compared to **19**, **25**, **27** with less number of clusters. Also note that in chromene derivatives, possibly the branching due to ring fusion with the chromene ring does not contribute to the activity as seen in compound **20**.

<S_{ssO}-5.9349>

The S_{ssO} descriptor belongs to the class of electro-topological state index, which includes both electronic and topological information, and it designates the sum of contribution for oxygens with two single bonds. The spline term $<S_{ssO}-5.93498>$ negatively contributes to the activity and it infers that there should be a limit for the number of such oxygens with two single bonds, such that the corresponding value of “ S_{ssO} ” remains less than 5.9349. Therefore, the compounds that are devoid of such oxygens (compound **6**) or compounds having one such oxygen (like in chromene moiety; compounds **1**, **2**, **9**) have good activity, but the presence of more number of such oxygen atoms is unfavorable for the activity as seen in compounds **17**, **23**, **25**. Especially, compounds having methoxy group at 3rd position to the chromene ring (**23**, **25**) and dioxole group (**17**) at 2nd position to the chromene ring are found to have low activity.

<0.20048-ETA_EtaP_L>

ETA_EtaP_L descriptor belongs to the class of ETA indices and is the highest contributing descriptor in the present model. This descriptor signifies local connectedness relative to the molecular size. It carries information related to branching, presence of heteroatom, and unsaturation. The spline term $<0.20048-ETA_EtaP_L>$ positively contributes to the activity, and it suggests that this descriptor (ETA_EtaP_L) can attain a maximum value of 0.20048, without affecting the activity. Therefore, according to this model, as the value of ETA_EtaP_L decreases below 0.20048, the value of the spline term (0.20048-ETA_EtaP_L) increases, and hence the contribution to the activity increases. The ETA term is highly correlated to the presence

of branching in a molecule, but relative to the molecular size. If the amount of branching is high relative to the molecular size, as seen in compounds **11**, **13**, **14**, **20**, **24** the value of $<0.20048\text{-ETA_EtaP_L}>$ will be low and so will be the activity values of these compounds. It seems that the subgraph count term (SC-3_C) is being balanced by the ETA term. Thus, both molecular size and branching are important for the activity.

Interpretation of pharmacophore studies

All the compounds were screened through the previously developed AChE pharmacophore model (Fig. 2) having 4 features, i.e., hydrogen bond acceptor (HBA1 and HBA2), hydrophobic aromatic, and hydrophobic aliphatic. 28 compounds of this data set showed only 2 features out of the required 4 features and two compounds (**5** and **19**) were not mapped. The chromene moiety acts as the main source for HBA feature and the phenyl group attached at 2nd position of chromene moiety acts as the hydrophobic aromatic feature.

Interpretation of results from docking studies

Docking studies of all the 30 compounds were carried out using the set docking protocol obtained from docking the co-crystal ligand. The RMSD between the original conformation of co-crystal ligand present in human AChE co-crystal structure (i.e., PDB: 4M0E) and the docked conformation of co-crystal ligand was found to be low, i.e., 0.41 Å and the docked pose also reproduced the intermolecular interactions that were reported in the co-crystal structure.

It is observed that the chromene moiety and the phenyl group attached at 2nd position to chromene moiety are involved in π - π interaction with Trp 286 and Tyr 341. The carbonyl group (chromene moiety) takes part in hydrogen bond with Ser 293, while the hydroxyl groups especially at 3rd position in chromen-4-one moiety take part in hydrogen bond formation with Phe 295 or Tyr 124 (Fig. 5).

Based on the appropriate descriptors in the developed equation, essential structural or pharmacophore features of the flavonoid molecules for showing appreciable AChEI activities were evaluated. The pharmacophore geometric fit values and docking scores of the investigated compounds are summarized in Table 2.

Understanding the relation between antioxidant and AChEI activities of flavonoid analogs—are flavonoid analogs with high antioxidant activity good AChE inhibitors?

It is reported that most of the bioactivities of flavonoid analogs are the results of their interactions with several

enzymes in living systems and their antioxidant activity (Leung et al. 2006; Jeong et al. 2007). The antioxidant activity of the flavonoids is dependent on their ability (i) to scavenge ROS and other toxic free radicals, (ii) to chelate redox active metal ions (e.g., Fe^{2+} and Cu^{2+}), and (iii) synergistic activity with other antioxidants. However, in all the cases, structural pattern of the flavonoids has great influence on their activity (Silva et al. 2002; Das et al. 2014; Kanakis et al. 2007; Jeong et al. 2007; Kanakis et al. 2009). Therefore, it is really interesting to study the effect of the structure of the flavonoids on their antioxidant activity which in turn may control their AChE inhibitory activity and thus their potential to be used as anti-AD drugs.

Antioxidant flavonoid analogs show wide-spectrum of beneficial effects, and in recent times, this class of compounds gained popularity as nutraceuticals. Most of the flavonoid analogs selected for the present study showed high DPPH (2,2-diphenyl-1-picrylhydrazyl) radicals scavenging antioxidant activity. In addition to these, flavonoids, we have also incorporated some of the standard antioxidant (**27–28**, **30**) (Table 1) in our study which partially resembles the flavonoid analogs in structure. However, no good correlation between the DPPH radical scavenging antioxidant and AChEI activities of the flavonoid analogs was observed. In general, flavones and iso-flavones were found to be better antioxidants as well as AChE inhibitors compared to chalcones. Presence of hydroxy group at 3-position of the flavone skeleton highly influenced the radical scavenging antioxidant activity, but AChE inhibitory activity of the flavones was mostly influenced by their conjugation pattern.

Conclusion

The fluorescence spectroscopic method was found to be highly useful and easy to understand the binding interaction between the antioxidant flavonoid analogs and AChE. The binding interaction between these two species was understood on the basis of the parameters, like K_{SV} , K_B , n , and EC_{50} values which were explored further to develop a QSAR model using GFA-spline technique. The selected descriptors in the final model provided useful insights about the structural requirements to improve the activity against AChE. Based on pharmacophore features, like hydrogen bond acceptor [HBA1, HBA2] activity, hydrophobic aliphatic and aromatic characters, novel compounds can be designed based on the flavonoid scaffolds that might show higher (predicted) potential as AChE inhibitors than the parent compounds. The comparison between AChE inhibitory and DPPH radical scavenging antioxidant activities of the flavonoid analogs was also done.

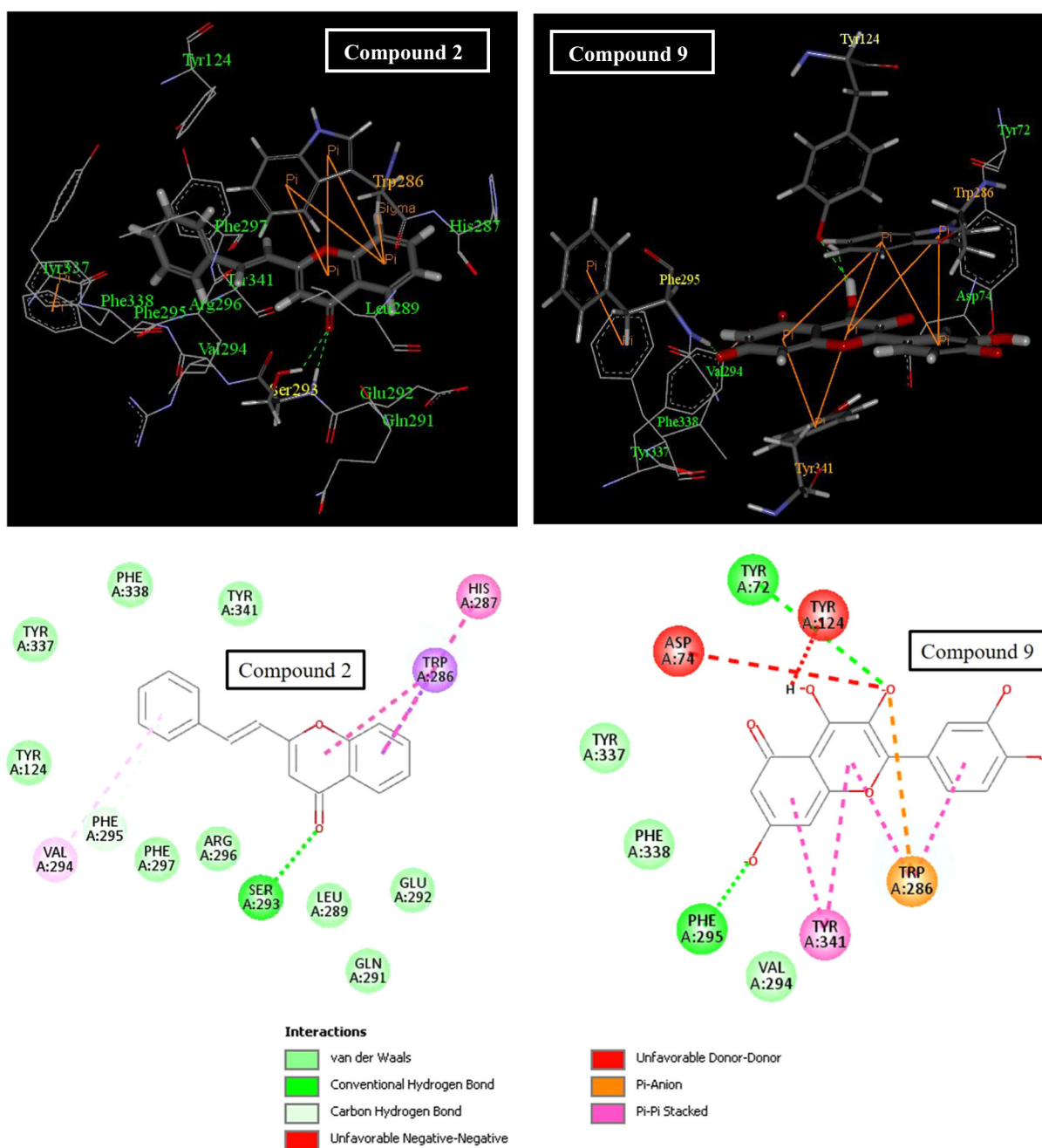


Fig. 5 Docked conformations of the flavonoid analogs, (*E*)-2-styryl-4H-chromone-4-one (compound 2) and quercetin (compound 9)

In future, this work can be explored further by synthesizing possibly newly designed compounds as well as additional flavonoid analogs based on the essential pharmacophoric and structural features as explored in the present study. These results can be exploited further to synthesize antioxidant flavonoid analogs, which might also act as potent AChE inhibitors. This will surely open up a new direction towards the development of potent and multifunctional AChE inhibitors based on these type of

nontoxic and bio-friendly flavonoid scaffolds, which might fight against the oxidative stress in living cells and prevent AD in elderly people.

Acknowledgements The authors thank the SERB-DST [Sanction Order No. SR/SO/BB-0007/2011 dated 21.08.2012 to NAB]. AK and TM thank UGC-CSIR (NET) and UGC-MANF, respectively for their fellowships. The authors thank the Department of Chemistry, Visva-Bharati and its DST-FIST and UGC-SAP (Phase-II) programs for necessary infrastructural and instrumental facilities.

Table 2 Pharmacophore and docking scores for the investigated 30 compounds

Compound ID	Dock score ^a	Fit value ^b (pharmacophore model)
1	81.478	3.601
2	82.846	3.140
3	82.009	3.571
4	77.941	1.509
5	79.225	0.000
6	92.292	3.098
7	92.522	3.577
8	87.520	3.644
9	103.311	3.583
10	98.742	3.739
11	93.542	3.724
12	81.970	3.644
13	99.132	3.739
14	94.667	3.728
15	92.125	3.665
16	81.932	3.617
17	92.095	3.708
18	90.487	3.718
19	80.925	0.000
20	84.834	3.558
21	89.008	3.158
22	82.218	3.655
23	83.690	3.693
24	98.659	3.737
25	83.650	3.688
26	131.033	3.727
27	68.261	3.091
28	67.643	2.337
29	102.918	3.708
30	72.966	3.719

^a**Dock scores** were obtained from the docking study (well described in respective section) using LigandFit docking module available in Discovery Studio software (Discovery Studio 2007). Here, the scores were computed using a consensus scoring function comprising 5 scoring functions that are as follows: LigScore1, LigScore2, Piecewise Linear Potential 1 (PLP1), Piecewise Linear Potential 2 (PLP2), Jain and Potential of mean force (PMF)

^b**Fit value** indicates how well the chemical sub-structures of a compound match the location constraints of the pharmacophoric features and their distance deviation from the feature centers (Rella et al. 2006)

Compliance with ethical standards

Conflict of interest The authors declare that they have no conflict of interest.

Publisher's note: Springer Nature remains neutral with regard to jurisdictional claims in published maps and institutional affiliations.

References

- Alam S, Mostahar S (2005) Studies of antimicrobial activity of two synthetic 2',4',6'-trioxygenated flavones. *J Appl Sci* 5:327–333
- Ambure P, Kar S, Roy K (2014) Pharmacophore mapping-based virtual screening followed by molecular docking studies in search of potential acetylcholinesterase inhibitors as anti-Alzheimer's agents. *Biosystems* 116:10–20
- Balasubramanian S, Nair MG (2000) An efficient “one pot” synthesis of isoflavones. *Synth Commun* 30:469–484
- Balkis A, Tran K, Lee YZ, Ng K (2015) Screening flavonoids for inhibition of acetylcholinesterase identified baicalein as the most potent inhibitor. *J Agric Sci* 7:26–35
- Bartolini M, Bertucci C, Cavrini V, Andrisano V (2003) beta-Amyloid aggregation induced by human acetylcholinesterase: inhibition studies *Biochem Pharmacol* 65:407–416
- Begum NA, Roy N, Laskar RA, Roy K (2011) Mosquito larvicidal studies of some chalcone analogues and their derived products: structure–activity relationship analysis. *Med Chem Res* 20:184–191
- Bera R, Sahoo BK, Ghosh KS, Dasgupta S (2008) Studies on the interaction of isoxazolcurcumin with calf thymus DNA. *Int J Biol Macromol* 42:14–21
- Brahmachari G, Choo CY, Ambure P, Roy K (2015) In vitro evaluation and in silico screening of synthetic acetylcholinesterase inhibitors bearing functionalized piperidine pharmacophores. *Bioorg Med Chem* 23:4567–4575
- Cerius2 Version 410 (2005) Accelrys, Inc., San Diego, CA
- ChemAxon Marvin Sketch 5115, Budapest, Hungary, <http://www.chemaxon.com/products.html>
- Chigurupati S, Selvaraj M, Mani V, Mohammad JI, Selvarajan KK, Akhtar SS, Marikannan M, Raj S, Teh LK, Salleh MZ (2018) Synthesis of azomethines derived from cinnamaldehyde and vanillin: in vitro acetylcholinesterase inhibitory, antioxidant and in silico molecular docking studies. *Med Chem Res* 27:807–816
- Das S, Ghosh S, Chattopadhyay N (2016) Unprecedented high fluorescence anisotropy in protic solvents: hydrogen bond induced solvent caging. *Chem Phys Lett* 644:284–287
- Das S, Mitra I, Batuta S, Alam MN, Roy K, Begum NA (2014) Design, synthesis and exploring the quantitative structure–activity relationship of some antioxidant flavonoid analogues. *Bioorg Med Chem Lett* 24:5050–5054
- Desideri N, Sestili I, Stein ML, Tramontano E, Corrias S, Colla PL (1998) Synthesis and anti-human immunodeficiency virus type 1 integrase activity of hydroxybenzoic and hydroxycinnamic acid flavon-3-yl esters. *Antivir Chem Chemother* 9:497–509
- Dhoubhadel SP, Tuladhar SM, Tuladhar SM, Wagley PP (1981) Synthesis of some 3-methoxyflavones and chromones. *Ind J Chem* 20:511–512
- Discovery Studio (2007) Version 2.5. Accelrys Software, San Diego, CA, USA
- Förstl H, Kurz A (1999) Clinical features of Alzheimer's disease. *Eur Arch Psychiatry Clin Neurosci* 249:288–290
- Furniss BS, Hannaford AJ, Rogers V, Smith PWG, Tatchell AR (1984) Vogel's text book of practical organic chemistry, 4th edn. John Wiley & Sons, New York
- Geissman TA (ed) (1962) The chemistry of flavonoid compounds. Pergamon Press, Oxford
- Gomes A, Fernandes E, Silva AMS, Pinto DCGA, Santos CMM, Cavaleiro JAS, Lima JLFC (2009) Anti-inflammatory potential of 2-styrylchromones regarding their interference with arachidonic acid metabolic pathways. *Biochem Pharmacol* 78:171–177
- Gunduz S, Goren, Ozturk AC, Ozturk T (2012) Facile syntheses of 3-hydroxyflavones. *Org Lett* 14:1576–1579

- Harborne JB, Mabry TJ (1982) The flavonoids: advances in research. Chapman and Hall, London
- Itoh M, Fujiwara Y, Sumitani M, Yoshihara K (1986) Mechanism of intramolecular excited-state proton transfer and relaxation processes in the ground and excited states of 3-hydroxyflavone and related compounds. *J Phys Chem* 90:5672–5678
- Jana B, Senapati S, Ghosh D, Bose D, Chattopadhyay N (2012) Spectroscopic exploration of mode of binding of ctDNA with 3-hydroxyflavone: a contrast to the mode of binding with flavonoids having additional hydroxyl groups. *J Phys Chem B* 116:639–645
- Jeong JM, Kang SK, Lee IH, Lee JY, Jung H, Choi CH (2007) Antioxidant and chemosensitizing effects of flavonoids with hydroxyl and/or methoxy groups and structure–activity relationship. *J Pharm Sci* 10:537–546
- Kamal A, Shaik AB, Reddy GN, Kumar CG, Joseph J, Kumar GB, Purushotham U, Sastry GN (2014) Synthesis, biological evaluation, and molecular modeling of (E)-2-aryl-5-styryl-1,3,4-oxadiazole derivatives as acetylcholinesterase inhibitors. *Med Chem Res* 23:2080–2092
- Kanakis CD, Nafisi S, Rajabi M, Shadaloi A, Tarantilis PA, Polissiou MG, Bariyanga J, Tajmir-Riahi HA (2009) Structural analysis of DNA and RNA interactions with antioxidant flavonoids. *Spectroscopy* 23:29–43
- Kanakis CD, Tarantilis PA, Polissiou MG, Diamantoglou S, Tajmir-Riahi HA (2007) An overview of DNA and RNA bindings to antioxidant flavonoids. *Cell Biochem Biophys* 49:29–36
- Koleva II, van Breek TA, Linssen JPH, Groot AD, Evstatieva LN (2002) Screening of plant extracts for antioxidant activity: a comparative study on three testing methods. *Phytochem Anal* 13:8–17
- Kung HF, Lee CW, Zhuang ZP, Kung MP, Hou C, Plössl K (2001) Novel stilbenes as probes for amyloid plaques. *J Am Chem Soc* 123:12740–12741
- Leung HWC, Kuo CL, Yang WH, Lin CH, Lee HZ (2006) Antioxidant enzymes activity involvement in luteolin induced human lung squamous carcinoma CH27 cell apoptosis. *Eur J Pharmacol* 534:12–18
- Li SY, Wang XB, Xie SS, Jiang N, Wang KDG, Yao HQ, Sun HB, Kong LY (2013) Multifunctional tacrine–flavonoid hybrids with cholinergic, β -amyloid-reducing, and metal chelating properties for the treatment of Alzheimer's disease. *Eur J Med Chem* 69:632–646
- Liu X, Chen X, Xiao J, Zhao J, Jiao F, Jiang X (2010) Effect of hydrogenation on ring C of flavonols on their affinity for bovine serum albumin. *J Solut Chem* 39:533–542
- Lu Y, Lv J, Zhang G, Wang G, Liu Q (2010) Interaction of an anthracycline disaccharide with ctDNA: investigation by spectroscopic technique and modeling studies. *Spectrochim Acta Part A* 75:1511–1515
- Luo W, Su YB, Hong C, Tian RG, Su LP, Wang YQ, Li Y, Yue JJ, Wang CJ (2013) Design synthesis and evaluation of novel 4-dimethylamine flavonoid derivatives as potential multi-functional anti-Alzheimer agents. *Bioorg Med Chem* 21:7275–7282
- Malisauskas R, Botyriute A, Cannon JG, Smirnovas V (2015) Flavone derivative as insulators of insulin amyloid-like fibril formation. *PLoS ONE* 10:e0121231
- Mauri A, Consonni V, Pavan M, Todeschini R (2006) Dragon software: an easy approach to molecular descriptor calculations. *Match* 56:237–248
- Mesulam MM, Guillozet A, Shaw P, Levey A, Duysen EG, Lockridge O (2002) Acetylcholinesterase knockouts establish central cholinergic pathways and can use butyrylcholinesterase to hydrolyze acetylcholine. *Neuroscience* 110:627–639
- Naik KN, Naik HB (1990) Synthesis of some chalcones and their antibacterial activity. *J Ind Chem Soc* 67:844–845
- Pietta PG (2000) Flavonoids as antioxidants. *J Nat Prod* 63:1035–1042
- Pinho BR, Ferreres F, Valentao P, Andrade PB (2013) Nature as source of metabolites with cholinesterase-inhibitory activity: an approach to Alzheimer's disease treatment. *J Pharm Pharmacol* 65:1681–1700
- Racchi M, Mazzuccelli M, Porrello E, Lanni C, Govoni S (2004) Acetylcholinesterase inhibitors: novel activities of old molecules. *Pharmacol Res* 50:441–451
- Rella M, Rushworth CA, Guy JL, Turner AJ, Langer T, Jackson RM (2006) Structure-based pharmacophore design and virtual screening for novel angiotensin converting enzyme 2 inhibitors. *J Chem Inf Model* 46:708–716
- Reyes AE, Chacón MA, Dinamarca MC, Cerpa W, Morgan C, Inestrosa NC (2004) Acetylcholinesterase–a complexes are more toxic than a fibrils in rat hippocampus: effect on rat-amyloid aggregation, laminin expression, reactive astrocytosis, and neuronal cell loss. *Am J Pathol* 164:2163–2174
- Ryu HW, Oh SR, Curtis-Long MJ, Lee JH, Song HH, Park KH (2014) Rapid identification of cholinesterase inhibitors from the seed-cases of mangosteen using an enzyme affinity assay. *J Agric Food Chem* 62:1338–1343
- Santillo MF, Liu Y (2015) A fluorescence assay for measuring acetylcholinesterase activity in rat blood and a human neuroblastoma cell line (SH-SY5Y). *J Pharmacol Toxicol Methods* 76:15–22
- Silva MM, Santos MR, Caroco G, Rocha R, Justino G, Mira L (2002) Structure–antioxidant activity relationships of flavonoids: a re-examination. *Free Radic Res* 36:1219–1227
- Sun M, Su M, Sun H (2018) Spectroscopic investigation on the interaction characteristics and inhibitory activities between baicalin and acetylcholinesterase. *Med Chem Res* 27:1589–1598
- Tyukavkina NA, Pogodaeva NN (1971) Ultraviolet absorption of flavonoids II. Ionization constants of 7- and 4'-hydroxy derivatives of flavone and flavonol. *Chem Nat Compd* 7:8–11
- Uriarte-Pueyo I, Calvo MI (2011) Flavonoids as acetylcholinesterase inhibitors. *Curr Med Chem* 18:5289–5302
- Vitorino J, Sottomayor MJ (2010) DNA interaction with flavones and hydroxyflavones. *J Mol Struct* 975:292–297
- Williams P, Sorribas A, Howes MJR (2011) Natural products as a source of Alzheimer's drug leads. *Nat Prod Rep* 28:48–77
- Xie Y, Yang W, Chen X, Xiao J (2014) Inhibition of flavonoids on acetylcholinesterase: binding and structure–activity relationship. *Food Funct* 5:2582–2589
- Yap CW (2011) PaDEL-descriptor: an open source software to calculate molecular descriptors and fingerprints. *J Comput Chem* 32:1466–1474
- Zhang S, Sun X, Jing Z, Qu F (2011) Spectroscopic analysis on the resveratrol–DNA binding interactions at physiological pH. *Spectrochim Acta Part A* 82:213–216